Proceedings of the Second International Workshop on
Fundamental Issues and Future Research Directions for Parallel Mechanisms and Manipulators
September 21–22, 2008, Montpellier, France
N. Andreff, O. Company, M. Gouttefarde, S. Krut and F. Pierrot, editors

Atlas Motion Platform Generalized Kinematic Model

M. JOHN D. HAYES
Department of Mechanical and Aerospace Engineering
Carleton University
Ottawa, Ontario, Canada, K1S 5B6
jhayes@mae.carleton.ca

ROBERT G. LANGLOIS
Department of Mechanical and Aerospace Engineering
Carleton University
Ottawa, Ontario, Canada, K1S 5B6
rlangloi@mae.carleton.ca

ABRAHAM WEISS
Department of Mechanical and Aerospace Engineering
Carleton University
Ottawa, Ontario, Canada, K1S 5B6
aweiss2@connect.carleton.ca

Abstract: *Conventional training simulators commonly use the hexapod configuration to provide motion cues. While widely used, studies have shown that hexapods are incapable of producing the range of motion required to achieve high fidelity simulation required in many applications. A novel alternative is the Atlas motion platform. This paper presents, for the first time, a general kinematic model of the platform which can be applied to any spherical platform actuated by three omnidirectional wheels. In addition, conditions for slip-free and singularity-free motions are identified. Two illustrative examples are given for different omnidirectional wheel configurations.*

1 Introduction

The Atlas motion platform (Hayes and Langlois, 2005) was introduced as a practical alternative to the Gough hexapod architecture (Gough, 1956; Stewart, 1965). A proof-of-concept table-top Atlas platform demonstrator is illustrated in Figure 1. In this architecture orienting is decoupled from positioning, and unbounded rotation is possible about any axis. The decoupling is accomplished by fixing a three degree of freedom spherical orienting platform on a linear platform with three orthogonal translational directions.

The key to the design is the use of three omnidirectional wheels which impart angular displacements to the sphere, thereby providing rotational actuation. The omnidirectional wheels used in the table-top demonstrator have two offset races of castor rollers on their periphery, see Figure 2. The omnidirectional wheel castor rollers provide near friction-free motion parallel to each omnidirectional wheel rotation axis. This feature creates the possibility for unbounded rotational displacements of the sphere.

The concept of a spherical actuator is not new. Spherical dc induction motors were introduced in 1959 in Williams *et al.* (1959). Developments continued over the next 30 years leading to designs presented in Roth and Lee (1995) and Chirikjian and Stein (1999), for example. However, due to physical limitations imposed by the stator and commutator, angular displacements are limited. Unbounded rotational motion is achieved by the Eclipse II architecture (Kim *et al.*, 2002), however its orientation workspace is constrained by structural interferences, and rotation limits of the spherical joints. Many designs for wheeled platforms exist, however changes in orientation all occur about vertical axes. For example, Lauwers *et al.* (2005) use friction wheels to roll a sphere along the ground, while Ferriere *et al.* (1998) use a single omnidirectional wheel to rotate a sphere about a single axis. Additionally, spherical linkages exist, Gosselin (1994) for example, but all have limited ranges of motion.

Since the Atlas sphere interacts with the omnidirectional wheels through simple contact, there are no joints or levers constraining its motion. This allows full 360° rotation about any axis in the workspace reachable by the sphere centre. The travel limits of the linear platform are bounded only by the length of the rails and dimensions of the scissor-jack. The result is a fully dexterous reachable workspace free from orienting joint limits, self-collisions, or self-interference of any kind. The only bounds on the workspace are the limits of reach of the sphere centre.

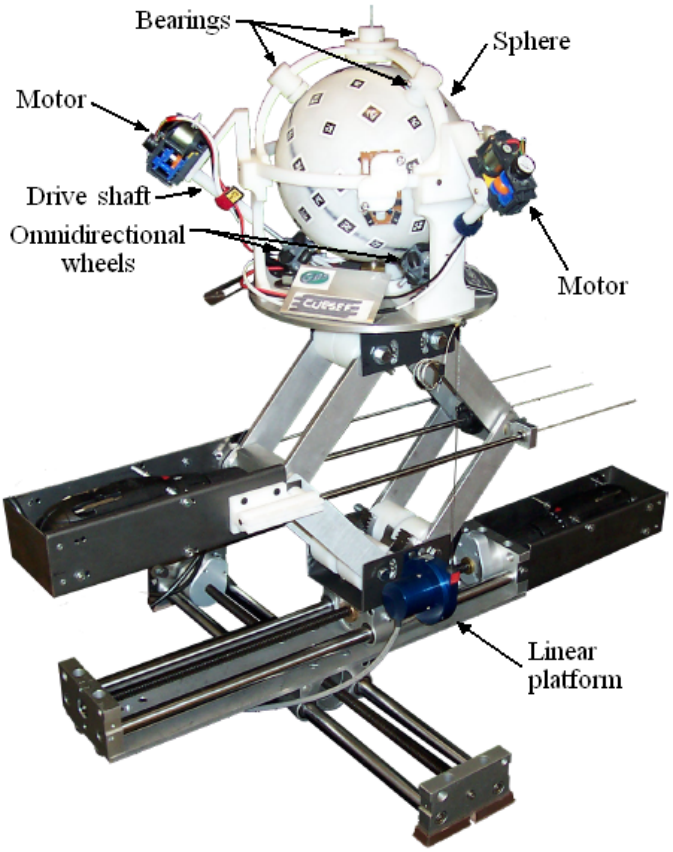

Figure 1: The Atlas table-top 6-DOF demonstrator highlighting the omnidirectional wheel actuation concept.

In this paper the kinematics of the Atlas motion platform are presented in a general form for the first time. The general kinematic model leads to a simple Jacobian whose elements are all time invariant. Because of the time invariance, design parameters may be selected such that the Jacobian is always invertible. As a result, the forward and inverse kinematics are always computable with a single matrix multiplication. Conditions for slip-free and singularity-free orienting capability are identified as well. These results underscore an unexpected strength of the architecture: computationally simple kinematics.

Two examples are given for different omnidirectional wheel configurations. The first example (Section 4.1) features an arrangement where the contact points of the omnidirectional wheels are located where the basis vectors of a sphere centred orthogonal inertial coordinate reference system pierce the sphere. The wheels are oriented such that individual wheel rotations produce angular displacements in yaw, pitch, and roll. The second example (Section 4.2) uses the original Atlas configuration outlined in Robinson *et al.* (2005).

The two examples serve to illustrate the elegance of the architecture, and the simplicity of the resulting kinematic model. They further serve to demonstrate that the current general model offers a substantial improvement over the earlier configuration specific kinematic models formulated by Holland *et al.* (2005) and Robinson *et al.* (2005).

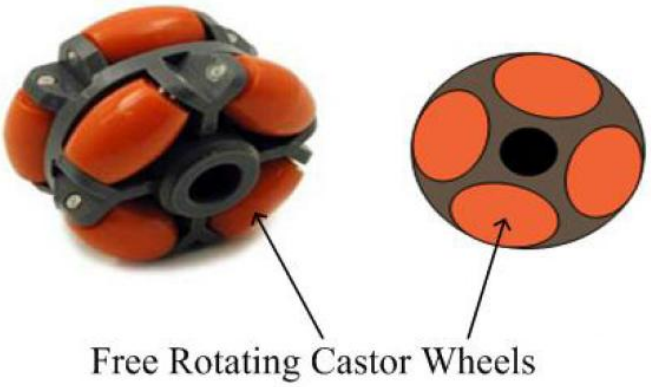

Figure 2: The omnidirectional wheel used in the Atlas prototype.

2 Applications

Simulator motion platforms require a high degree of repeatability for high fidelity. Moreover, platform motions must be precisely timed with the graphics to avoid simulator sickness. Traditionally, hexapods have been used. This is because of the commonly held belief that they offer significantly higher payload to weight ratios than serial kinematic chains. The primary application of the Atlas motion platform is motion simulation. A simulated vehicle cockpit would be housed within the sphere. Projection facilities would also be internal to the sphere. The ability to produce continuous unlimited angular displacements in any combination of roll, pitch, and yaw puts Atlas in new territory in terms of freedom of motion for such mechanical devices.

The Atlas platform was originally designed to offer similar stiffness as hexapods, but to have a larger workspace and simplified kinematics. Features of the design, primarily relating to the expanded range of motion, have lead to a broader range of applications than the positioning and pointing tasks assigned to hexapods. For example, hardware-in-the-loop simulation of satellite sensor packages could be performed for manoeuvres as complex as variable-axis tumbles. Basic physiological research could benefit from the large available range of motion for investigating issues such as debilitating simulator sickness. Entertainment applications include home gaming centers with a motion platform. Diverse vehicle motions could be simulated: on and off road vehicles; fixed and rotary wing aircraft; roller-coaster rides. Additional applications, and sometimes associated challenges, will continue to emerge as the Atlas concept is developed.

3 Generalized Atlas Kinematics

Generalization of the Atlas platform kinematics is achieved by defining the orienting platform as a sphere actuated by three omnidirectional wheels with arbitrary sphere contact point locations and arbitrary actuation directions. While design optimization to achieve economic and performance goals will follow from this generalized formulation, it will not be addressed in this paper.

The issue of slip at the interface between the sphere and each omnidirectional wheel is crucial for position level control

and must be addressed in formulating the generalized kinematic model. Kinematic slip is defined as the difference between the velocity $\mathbf{V}_i$ induced by actuating wheel i at its contact point with the sphere and the velocity $\mathbf{V}'_i$ of the corresponding contact point on the sphere (Holland *et al.*, 2005). Kinematic slip must be absent in order to achieve zero slip in the system. This is termed the *kinematic slip condition*. However, zero slip due to kinetic reasons can always be obtained by using ball bearings to transmit an externally applied constraint force large enough to create normal forces at the contact points which generate friction forces at the same contact points large enough to overcome the resulting inertial forces. The same is true with respect to ensuring kinematic closure, i.e., that there is never loss of contact between the sphere and the omnidirectional wheels. This is achieved for the Atlas demonstrator, shown in Figure 1, through the use of variable load-inducing bearings. The theoretical kinematics problem then becomes that of determining conditions which ensure the kinematic slip condition is satisfied for the three omnidirectional wheels and sphere.

Here it is important to observe that the omnidirectional wheels used in the Atlas platform allow free rolling perpendicular to the actuation direction (Leow *et al.*, 2002; Angeles, 2003), hence the kinematic slip condition in this direction is relaxed. This means that the velocity component in this direction is unknown. While a generalized approach to determining the instantaneous screw, using the velocities of three points on a rigid body, exists (Angeles, 2003, 1988), it requires complete knowledge of these velocities. That is, the three components of the velocity for each given point must be known. Because of the relaxation of the kinematic slip condition in the free-roll direction, only two components of the velocity at each contact point are known. Hence the instantaneous screw based method may not be immediately used for the Atlas sphere.

3.1 Kinematic Model

In the Atlas Platform architecture, translational displacements generated with the XYZ linear platform are completely decoupled from the rotational displacements of the sphere. Modelling the linear velocity of the geometric centre of the sphere is straightforward and well understood and represented as a simple linear term which must be added to the more demanding spherical kinematic model. Therefore, without loss in generality, only the spherical kinematics will be considered here. An arbitrarily general configuration is assumed, and an inertial coordinate frame is positioned at the geometric centre of the sphere, as illustrated in Figure 3. The omnidirectional wheels are treated as ideal. This means that the location of the contact point is invariant with respect to the inertial coordinate frame. The change in contact point due to omnidirectional wheel design, such as dual-row omnidirectional wheels, is beyond the scope of this paper. However, the effect of the changing contact point leads to a set of simple, constant correction matrices (Weiss *et al.*, 2008) that pre-multiply the Jacobian derived in this paper.

All geometric developments presented here are referenced to the inertial coordinate frame. The $\mathbf{R}_i$ are the position vectors of the contact points and $\mathbf{\Omega}$ is the angular velocity vector of the

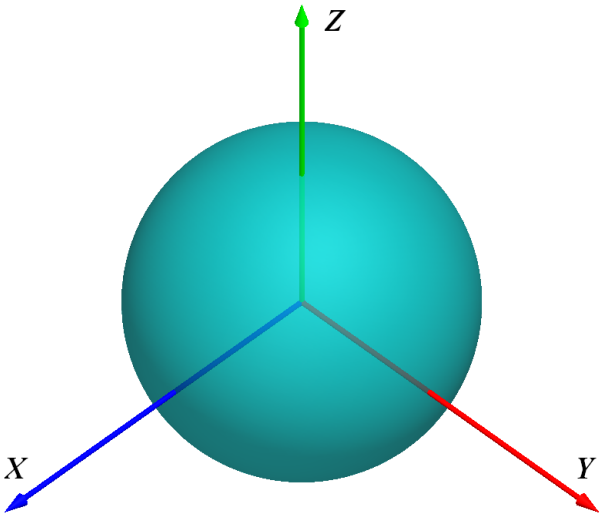

Figure 3: Inertial coordinate frame with origin at the geometric centre of the sphere.

sphere. The linear velocity of the contact point on the sphere side of the sphere/omnidirectional wheel interface is given by

$$\mathbf{V}'_i = \mathbf{\Omega} \times \mathbf{R}_i, \tag{1}$$

where subscript $i \in \{1, 2, 3\}$ refers to a specific omnidirectional wheel. The linear velocity of the contact point on the omnidirectional wheel side can be decomposed into two components: one in the actuation direction, and one transverse component in the direction of the free-roll of the castors:

$$\mathbf{V}_i = V_{ai}\hat{\mathbf{v}}_{ai} + V_{ri}\hat{\mathbf{v}}_{ri}, \tag{2}$$

where $\hat{\mathbf{v}}_{ai}$ is a unit vector in the actuation direction, V_{ai} is its magnitude, $\hat{\mathbf{v}}_{ri}$ is a unit vector in the free-roll direction, and V_{ri} is its magnitude. These two vectors are orthogonal, and hence the following condition must be satisfied:

$$\hat{\mathbf{v}}_{ai} \cdot \hat{\mathbf{v}}_{ri} = 0. \tag{3}$$

The kinematic slip condition may now be expressed as:

$$(\mathbf{\Omega} \times \mathbf{R}_i) \cdot \hat{\mathbf{v}}_{ai} = V_{ai}. \tag{4}$$

Equation 4 may be stated in words as *the velocity in the actuation direction of a contact point on the sphere is required to be the same as that of the corresponding contact point on the associated omnidirectional wheel in the same direction*. If Equation 4 is satisfied then slip is absent and the kinematic slip condition is satisfied. Equation (4) can be rearranged using some well known vector product relations as:

$$(\mathbf{\Omega} \times \mathbf{R}_i) \cdot \hat{\mathbf{v}}_{ai} = (\mathbf{R}_i \times \hat{\mathbf{v}}_{ai}) \cdot \mathbf{\Omega} = V_{ai}. \tag{5}$$

Since the magnitude of all position vectors is the radius of the sphere, R, the position vectors of the contact points can be written as

$$\mathbf{R}_i = R\hat{\mathbf{R}}_i, \tag{6}$$

where $\hat{\mathbf{R}}_i$ is a unit vector in the direction of the contact point from the sphere centre. Equation (5) can then be rewritten as

$$(\hat{\mathbf{R}}_i \times \hat{\mathbf{v}}_{ai}) \cdot \boldsymbol{\Omega} = \frac{V_{ai}}{R}. \tag{7}$$

The actuation velocity of the omnidirectional wheel may be expressed as:

$$V_{ai}\hat{\mathbf{v}}_{ai} = \boldsymbol{\omega}_i \times \mathbf{r}_i, \tag{8}$$

where $\boldsymbol{\omega}_i$ is the angular velocity vector of omnidirectional wheel i, and $\mathbf{r}_i$ is the vector emanating from the omnidirectional wheel centre to its contact point with the sphere. The magnitude of the contact point actuation velocity, V_{ai} can be expressed as the product of the magnitudes of $\boldsymbol{\omega}_i$ and $\mathbf{r}_i$:

$$V_{ai} = \omega_i r_i. \tag{9}$$

Hence,

$$(\hat{\mathbf{R}}_i \times \hat{\mathbf{v}}_{ai}) \cdot \boldsymbol{\Omega} = \frac{r_i}{R}\omega_i. \tag{10}$$

The corresponding induced unit angular velocities, $\hat{\boldsymbol{\Omega}}_i$, are defined to be

$$\hat{\boldsymbol{\Omega}}_i = \hat{\mathbf{R}}_i \times \hat{\mathbf{v}}_{ai}. \tag{11}$$

Substituting Equation (11) into Equation (10) yields

$$\hat{\boldsymbol{\Omega}}_i \cdot \boldsymbol{\Omega} = \frac{r_i}{R}\omega_i. \tag{12}$$

Equation (12) defines the relationship between the angular velocity of the sphere, $\boldsymbol{\Omega}$, and the actuation angular velocities of the omnidirectional wheels, ω_i. Populating Equation (12) for each of the three omnidirectional wheels leads, in essence, to the Jacobian of the system. However, this is not the precise mathematical definition that will be used to define the Jacobian. Regardless, this mapping between velocities remains useful as long as the system of three equations represented by Equation (12) possesses a real solution. Rewriting Equation (12) in component form for each omnidirectional wheel leads to:

$$\begin{bmatrix} \hat{\boldsymbol{\Omega}}_1^T \\ \hat{\boldsymbol{\Omega}}_2^T \\ \hat{\boldsymbol{\Omega}}_3^T \end{bmatrix} \begin{Bmatrix} \Omega_x \\ \Omega_y \\ \Omega_z \end{Bmatrix} = \frac{1}{R} \begin{bmatrix} r_1 & 0 & 0 \\ 0 & r_2 & 0 \\ 0 & 0 & r_3 \end{bmatrix} \begin{Bmatrix} \omega_1 \\ \omega_2 \\ \omega_3 \end{Bmatrix}. \tag{13}$$

The *induced unit angular velocity matrix*, $\hat{\boldsymbol{\Omega}}$, is defined to be

$$\hat{\boldsymbol{\Omega}} \;=\; \begin{bmatrix} \hat{\boldsymbol{\Omega}}_1 & \hat{\boldsymbol{\Omega}}_2 & \hat{\boldsymbol{\Omega}}_3 \end{bmatrix}. \tag{14}$$

Given the finite limits for dimensions of a real platform, the only way for Equation (13) to be inconsistent and possess no finite solution is if the transpose of the induced unit angular velocity matrix, $\hat{\boldsymbol{\Omega}}^T$, is rank deficient. This is a restatement of the expression for the kinematic slip condition. In order for the induced unit angular velocity matrix to retain full rank requires that the three unit vectors $\hat{\boldsymbol{\Omega}}_i$ be linearly independent. If this is true the kinematic slip condition will be satisfied and the system will be enabled to have zero slip in every orientation.

The Jacobian is, by definition, a mapping between time rates of change. By convention in robotics it is the mapping between the time rates of change of the joint variables to the time rates of change of the position and orientation of the end effector. The orienting Jacobian of the generalized Atlas architecture is derived by rewriting Equation (13) in the following way:

$$\boldsymbol{\Omega} = \frac{1}{R} \begin{bmatrix} \hat{\boldsymbol{\Omega}}_1^T \\ \hat{\boldsymbol{\Omega}}_2^T \\ \hat{\boldsymbol{\Omega}}_3^T \end{bmatrix}^{-1} \begin{bmatrix} r_1 & 0 & 0 \\ 0 & r_2 & 0 \\ 0 & 0 & r_3 \end{bmatrix} \begin{Bmatrix} \omega_1 \\ \omega_2 \\ \omega_3 \end{Bmatrix}. \tag{15}$$

Equation (15) relates the angular velocity of the sphere to the three angular velocity inputs of the actuating omnidirectional wheels. The terms which pre-multiply the omnidirectional wheel angular velocities represent the Jacobian. Hence, the generalized Atlas Jacobian is defined such that

$$\boldsymbol{\Omega} = \mathbf{J}\boldsymbol{\omega}, \tag{16}$$

where the magnitudes of the individual omnidirectional wheel angular velocities are collected in the array

$$\boldsymbol{\omega} = \left\{ \; \omega_1 \; \omega_2 \; \omega_3 \; \right\}^T. \tag{17}$$

Therefore, the Atlas Jacobian is defined to be:

$$\mathbf{J} = \frac{1}{R} \begin{bmatrix} \hat{\boldsymbol{\Omega}}_1^T \\ \hat{\boldsymbol{\Omega}}_2^T \\ \hat{\boldsymbol{\Omega}}_3^T \end{bmatrix}^{-1} \begin{bmatrix} r_1 & 0 & 0 \\ 0 & r_2 & 0 \\ 0 & 0 & r_3 \end{bmatrix}. \tag{18}$$

Inspection of the system Jacobian defined by Equation (18) reveals that unlike typical manipulator Jacobians, J is time invariant and depends only on design constants. Hence, these constants can be chosen such that the Jacobian has full rank so that the orienting workspace of the sphere is configurationally singularity free. Moreover, because the sphere can have any orientation, the reachable workspace is fully dexterous!

Because the Jacobian of the system is time invariant and constant, once the configuration has been determined, acceleration-level kinematics can be obtained by simple differentiation of the expression to obtain:

$$\dot{\boldsymbol{\Omega}} = \mathbf{J}\dot{\boldsymbol{\omega}} \tag{19}$$

Obtaining the expression for the orientation of the platform, however, is not as simple. This can be accomplished in several ways. In this work quaternions, or Euler parameters, are used because the unbounded and singularity-free nature of the design calls for a singularity-free representation. Integration of the quaternionic differential equation is required (Schwab *et al.*, 2006):

$$\dot{q} = \frac{1}{2}\Omega \circ q, \tag{20}$$

where q is the unit quaternion describing the orientation of the system, and $\Omega \circ q$ is a quaternionic product.

Finally, the inverse kinematics of the Atlas platform architecture are straightforward using the generalized kinematic model.

At the velocity level, the inverse kinematics problem may be stated as *determine the magnitudes of the individual omnidirectional wheel angular velocities required to attain a prescribed sphere angular velocity*. Owing to the simplicity of the generalized kinematic model all that is required is to invert Equation (16):

$$\boldsymbol{\omega} = \mathbf{J}^{-1}\boldsymbol{\Omega}, \tag{21}$$

where

$$\mathbf{J}^{-1} = R \begin{bmatrix} \frac{1}{r_1} & 0 & 0 \\ 0 & \frac{1}{r_2} & 0 \\ 0 & 0 & \frac{1}{r_3} \end{bmatrix} \begin{bmatrix} \hat{\boldsymbol{\Omega}}_1^T \\ \hat{\boldsymbol{\Omega}}_2^T \\ \hat{\boldsymbol{\Omega}}_3^T \end{bmatrix}. \tag{22}$$

4 Examples

Two velocity level kinematics examples with different arrangements of omnidirectional wheels illustrating the generality of the kinematic model are now presented. The first example features an arrangement where the contact points are located at the piercing points of the inertial coordinate reference system basis vectors. The actuation directions are selected such that changes in orientation of one wheel, while the other two remain stationary, produce sphere rotations about one of the basis vector directions. These rotations can be defined as yaw, pitch, and roll. The second example illustrates the new generalized kinematic model applied to the original Atlas configuration (Hayes and Langlois, 2005).

4.1 Orthogonal Omnidirectional Wheel Configuration

This example illustrates an orthogonal arrangement of omnidirectional wheels such that each contact point with the sphere is located on the piercing point of one of the inertial coordinate reference system basis vector directions. The omnidirectional wheels are oriented such that when two of the wheels are held fixed, rotations of the remaining wheel produce sphere rotations about one of the basis vectors. As illustrated by Figure 4, rotations of the omnidirectional wheel whose contact point is on the X-axis produce sphere rotations about the Y-axis; rotations of the omnidirectional wheel whose contact point is on the Y-axis produce sphere rotations about the Z-axis; rotations of the omnidirectional wheel whose contact point is on the Z-axis produce sphere rotations about the X-axis. This configuration of the three omnidirectional wheels leads to the kinematic slip condition being satisfied in every orientation of the sphere.

All vectors in the following discussion are referenced to the inertial coordinate system shown in Figure 4. The velocity level kinematics are completely described by populating the Jacobian defined by Equation (18). The orientation level and acceleration level kinematics can then be determined using Equations (20) and (19), respectively.

The basis direction vectors for the coordinate axes $\{X, Y, Z\}$ are $\{\hat{\mathbf{i}}, \hat{\mathbf{j}}, \hat{\mathbf{k}}\}$. The sphere contact points of omnidirectional wheel $\{1, 2, 3\}$ are located on the piercing points of basis direction vectors $\{\hat{\mathbf{i}}, \hat{\mathbf{j}}, \hat{\mathbf{k}}\}$, respectively. The sphere has radius R and each of the omnidirectional wheels have identical radii, so $r_1 = r_2 = r_3 = r$. Now all that remains is to populate the unit induced angular velocity matrix whose elements are defined by Equation (11).

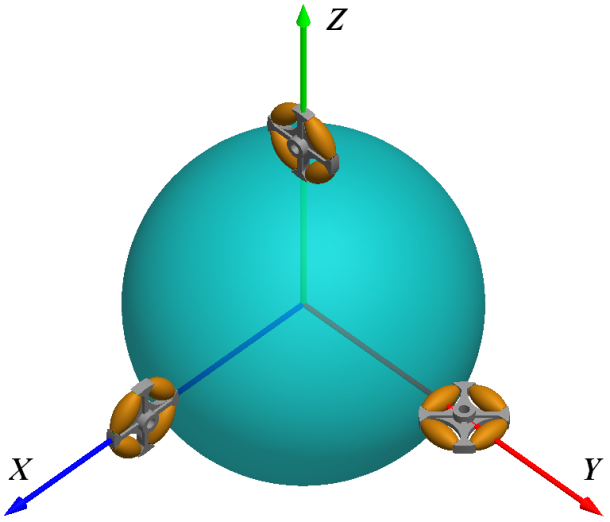

Figure 4: Kinematic architecture for the orthogonal case.

In order to accomplish this cross products are required of the unit position vectors of the sphere contact points and the unit induced linear velocity vectors in the actuation direction of the omnidirectional wheels, all relative to the sphere centre. The position vectors of the three sphere contact points are:

$$\mathbf{R}_1 = R\hat{\mathbf{i}};\ \mathbf{R}_2 = R\hat{\mathbf{j}};\ \mathbf{R}_3 = R\hat{\mathbf{k}}.$$

The corresponding unit vectors are:

$$\begin{aligned} \hat{\mathbf{R}}_1 &= [1,0,0]^T; \\ \hat{\mathbf{R}}_2 &= [0,1,0]^T; \\ \hat{\mathbf{R}}_3 &= [0,0,1]^T. \end{aligned}$$

Positive omnidirectional wheel rotations obey the right-hand-rule. That is, rotations of each omnidirectional wheel in the positive sense induce associated linear velocity components in the positive direction of the associated basis vector. Examining Figure 4 it is evident that induced unit linear velocity vectors are:

$$\begin{aligned} \hat{\mathbf{v}}_{a1} &= [0,0,1]^T; \\ \hat{\mathbf{v}}_{a2} &= [1,0,0]^T; \\ \hat{\mathbf{v}}_{a3} &= [0,1,0]^T. \end{aligned}$$

The cross products required by Equation (11) can now be evaluated and yield:

$$\begin{aligned} \hat{\boldsymbol{\Omega}}_1 &= \begin{bmatrix} 1 \\ 0 \\ 0 \end{bmatrix} \times \begin{bmatrix} 0 \\ 0 \\ 1 \end{bmatrix} = \begin{bmatrix} 0 \\ -1 \\ 0 \end{bmatrix}; \\ \hat{\boldsymbol{\Omega}}_2 &= \begin{bmatrix} 0 \\ 1 \\ 0 \end{bmatrix} \times \begin{bmatrix} 1 \\ 0 \\ 0 \end{bmatrix} = \begin{bmatrix} 0 \\ 0 \\ -1 \end{bmatrix}; \\ \hat{\boldsymbol{\Omega}}_3 &= \begin{bmatrix} 0 \\ 0 \\ 1 \end{bmatrix} \times \begin{bmatrix} 0 \\ 1 \\ 0 \end{bmatrix} = \begin{bmatrix} -1 \\ 0 \\ 0 \end{bmatrix}. \end{aligned}$$

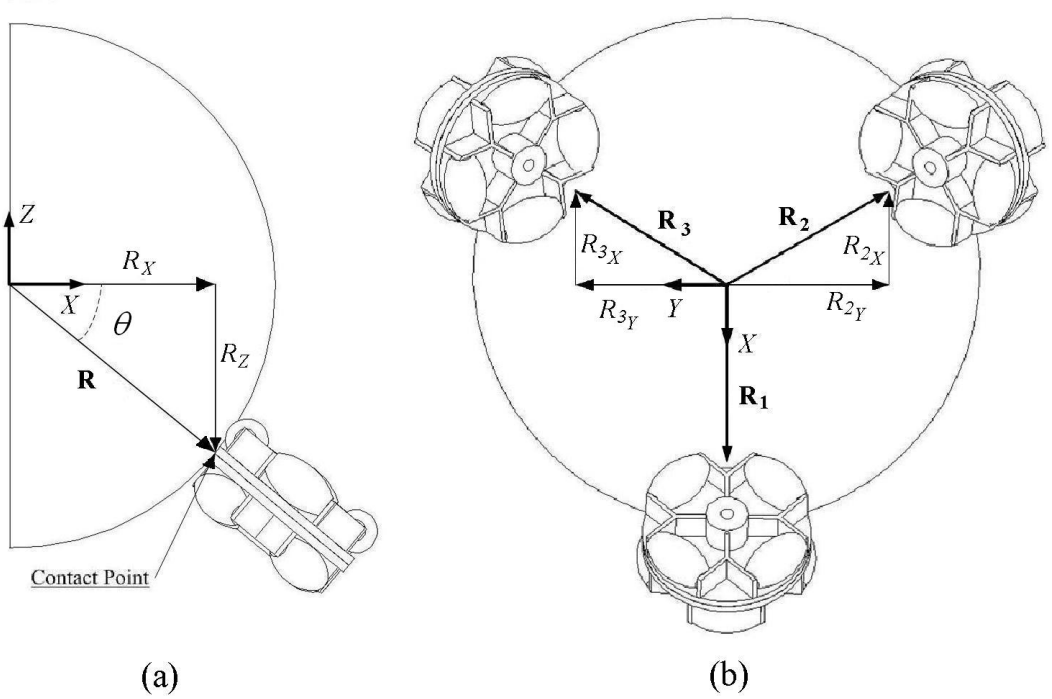

Figure 5: Configuration of the original Atlas spherical platform.

Hence

$$\hat{\mathbf{\Omega}}^T = \begin{bmatrix} 0 & -1 & 0 \\ 0 & 0 & -1 \\ -1 & 0 & 0 \end{bmatrix},$$

and

$$(\hat{\mathbf{\Omega}}^T)^{-1} = \begin{bmatrix} 0 & 0 & -1 \\ -1 & 0 & 0 \\ 0 & -1 & 0 \end{bmatrix}.$$

In this case $\hat{\mathbf{\Omega}} = (\hat{\mathbf{\Omega}}^T)^{-1}$, but in general this is not the case. Substituting these results directly into Equation (18) yields

$$\mathbf{J} = \frac{r}{R}\begin{bmatrix} 0 & 0 & -1 \\ -1 & 0 & 0 \\ 0 & -1 & 0 \end{bmatrix}. \quad (23)$$

Note the pleasing simplicity of the Jacobian expressed by Equation (23). Because its elements are all time invariant a quick examination by inspection reveals the unbounded and singularity free orienting workspace. Moreover, the rows are all linearly independent, and hence the kinematic slip condition is satisfied in every orientation. This is so because the induced unit angular velocity matrix, $\hat{\mathbf{\Omega}}$, always possesses full rank.

4.2 The Original Atlas Configuration

The original configuration of the Atlas motion platform (Hayes and Langlois, 2005) has the three omnidirectional wheels arranged on the edges of an equilateral triangle giving an angular separation of 120° in the XY-plane, see Figure 5(b). The elevation angle of each omnidirectional wheel relative to the XY-plane is 40°. The reason for the equilateral configuration is to achieve even force and torque distribution on the omnidirectional wheels, however the elevation angle of 40° was selected for ease of manufacturing and assembly. To generalize this equilateral configuration an arbitrary elevation angle θ is used, and illustrated in Figure 5(a).

In this case

$$\begin{aligned} \hat{\mathbf{R}}_1 &= [\cos\theta, 0, -\sin\theta]^T, \\ \hat{\mathbf{R}}_2 &= \frac{1}{2}\left[-\cos\theta, -\sqrt{3}\cos\theta, -2\sin\theta\right]^T, \\ \hat{\mathbf{R}}_3 &= \frac{1}{2}\left[-\cos\theta, \sqrt{3}\cos\theta, -2\sin\theta\right]^T. \end{aligned}$$

The induced unit linear velocity vectors in the actuation directions are:

$$\begin{aligned} \hat{\mathbf{v}}_{a1} &= [0, -1, 0]^T; \\ \hat{\mathbf{v}}_{a2} &= \frac{1}{2}\left[-\sqrt{3}, 1, 0\right]^T; \\ \hat{\mathbf{v}}_{a3} &= \frac{1}{2}\left[\sqrt{3}, 1, 0\right]^T. \end{aligned}$$

The cross products required by Equation (11) can now be

evaluated and yield:

$$\hat{\boldsymbol{\Omega}}_{\mathbf{1}} = \begin{bmatrix} \cos\theta \\ 0 \\ -\sin\theta \end{bmatrix} \times \begin{bmatrix} 0 \\ -1 \\ 0 \end{bmatrix} = \begin{bmatrix} -\sin\theta \\ 0 \\ -\cos\theta \end{bmatrix};$$

$$\hat{\boldsymbol{\Omega}}_{\mathbf{2}} = \frac{1}{2}\begin{bmatrix} -\cos\theta \\ -\sqrt{3}\cos\theta \\ -2\sin\theta \end{bmatrix} \times \frac{1}{2}\begin{bmatrix} -\sqrt{3} \\ 1 \\ 0 \end{bmatrix} = \frac{1}{2}\begin{bmatrix} \sin\theta \\ \sqrt{3}\sin\theta \\ -2\cos\theta \end{bmatrix};$$

$$\hat{\boldsymbol{\Omega}}_{\mathbf{3}} = \frac{1}{2}\begin{bmatrix} -\cos\theta \\ \sqrt{3}\cos\theta \\ -2\sin\theta \end{bmatrix} \times \frac{1}{2}\begin{bmatrix} \sqrt{3} \\ 1 \\ 0 \end{bmatrix} = \frac{1}{2}\begin{bmatrix} \sin\theta \\ -\sqrt{3}\sin\theta \\ -2\cos\theta \end{bmatrix}.$$

Hence

$$\hat{\boldsymbol{\Omega}}^T = \begin{bmatrix} -\sin\theta & 0 & -\cos\theta \\ \frac{1}{2}\sin\theta & \frac{\sqrt{3}}{2}\sin\theta & -\cos\theta \\ \frac{1}{2}\sin\theta & -\frac{\sqrt{3}}{2}\sin\theta & -\cos\theta \end{bmatrix},$$

and

$$(\hat{\boldsymbol{\Omega}}^T)^{-1} = \frac{1}{3}\begin{bmatrix} -2\csc\theta & \csc\theta & \csc\theta \\ 0 & \sqrt{3}\csc\theta & -\sqrt{3}\csc\theta \\ -\sec\theta & -\sec\theta & -\sec\theta \end{bmatrix}.$$

It is clear that if a square matrix is rank deficient, then its inverse will also be rank deficient. The matrix will lose full rank if it's determinant vanishes, and it will no longer be invertible. If $\hat{\boldsymbol{\Omega}}^T$ is invertible, then

$$\det \hat{\boldsymbol{\Omega}}^T = \frac{1}{\det (\hat{\boldsymbol{\Omega}}^T)^{-1}} = \frac{3}{2}\sqrt{3}\cos\theta\sin\theta^2.$$

While the unit induced angular velocity matrix contains no time varying terms, the design parameter θ can be chosen such that it will become rank deficient. It is easy to see that $\hat{\boldsymbol{\Omega}}^T$, as well as $(\hat{\boldsymbol{\Omega}}^T)^{-1}$ possess two such values, namely $\theta = \pi/2$ or $\theta = 0$. The Jacobian can be evaluated for all other values of θ sufficiently different from the limiting values. For this configuration of omnidirectional wheels the resulting Jacobian is:

$$\mathbf{J} = \frac{r}{3R}\begin{bmatrix} -2\csc\theta & \csc\theta & \csc\theta \\ 0 & \sqrt{3}\csc\theta & -\sqrt{3}\csc\theta \\ -\sec\theta & -\sec\theta & -\sec\theta \end{bmatrix}. \qquad (24)$$

This result is in agreement with those reported by Robinson *et al.* (2005) and Holland *et al.* (2005).

If the design parameter θ is suitably chosen then the kinematic slip condition will be satisfied for every orientation of the sphere, and the mechanical system will be enabled to have zero slip. As is the case for the orthogonal configuration in Section 4.1, this is so because the induced unit angular velocity matrix, $\hat{\boldsymbol{\Omega}}$, always possesses full rank.

5 Conclusions

In this paper a novel generalized kinematic model for the Atlas spherical platform has been presented. The model is formulated at the velocity level, and is based on orthogonal decomposition of actuation and free rolling velocities of the castors on the three omnidirectional wheels. The kinematic model is general, and a significant improvement of that presented by Robinson *et al.* (2005) and Holland *et al.* (2005) because it can be applied to any arrangement of three omnidirectional wheels that result in three orientational degrees-of-freedom. The utility and simplicity of the model is demonstrated with two examples.

An important result of this work is the identification of the kinematic slip condition, which is a necessary condition for eliminating kinematic slip, and should be used in the detail design phase of such motion platforms. The kinematic slip condition is simply that the three omnidirectional wheel-induced angular velocity direction vectors $\hat{\boldsymbol{\Omega}}_i$ must be linearly independent. This means that the singularities and slip issues that result from kinematic sources may be eliminated at the design stage, rather than relying on real-time control solutions. The simplicity of the generalized kinematic model of the platform will be advantageous when it comes to formulating a motion control system and the associated real-time computations required.

These results do not eliminate the need to evaluate and minimize kinetically-induced slip, i.e., slip that results from contact forces and moments. Rather, the formulation presented herein reveals necessary conditions which lead to kinematic slip-free configurations of omnidirectional wheels. Design optimization of such platforms can be approached using these results for practical criteria. For example, elimination of kinetically-induced slip, minimization of reaction forces, or actuation power requirements could serve as design optimization criteria.

References

J. Angeles, 2003, *Fundamentals of Robotic Mechanical Systems: Theory, Methods, and Algorithms, 2nd ed.*, Springer-Verlag, New York, NY, USA.

J. Angeles, 1988, *Rational Kinematics*, Springer-Verlag, New York, NY, USA.

G.S. Chirikjian and D. Stein, 1999, "Kinematic Design and Commutation of a Spherical Stepper Motor", *IEEE/ASME Transactions on Mechatronics*, vol. 4, no. 4, pp. 342-353.

L. Ferriere, B. Raucent, May 1998 "ROLLMOBS, a New Universal Wheel Concept", *Proceedings of the 1998 IEEE International Conference on Robotics and Automation*, pp. 1877-1882.

C. Gosselin, J.F. Hamel, 1994, The agile eye: a high performance three-degree-of-freedom camera-orienting device, *IEEE Int. conference on Robotics and Automation*, pp.781-787.

V.E. Gough, 1956, "Contribution to Discussion of Papers on Research in Automobile Stability, Control and Tyre Performance", *Proc of Auto Div. Inst. Mech. Eng.*, pp. 392-394.

M.J.D. Hayes, R.G. Langlois, 2005, "A Novel Kinematic Architecture for Six DOF Motion Platforms", *CSME Transactions, Special Edition*, vol. 29, no. 4, pp. 701-709.

J.B. Holland, M.J.D. Hayes, and R.G. Langlois, 2005, "A Slip Model for the Spherical Actuation of the Atlas Motion Platform", *CSME Transactions, Special Edition*, vol. 29, no. 4, pp. 711-720.

J. Kim, J.C. Hwang, J.S. Jim, C.C. Iurascu, F.C. Park, Y.M. Cho, June 2002, "Eclipse II: A New Parallel Mechanism Enabling Continuous 360-Degree Spinning Plus Three-Axis Translational Motions", *IEEE Transactions on Robotics and Automation*, vol. 18, no. 3, pp. 367-373.

T.B. Lauwers, G.A. Kantor, R.L. Hollis, October 2005, "One is Enough!", *Proceedings of 2005 International Symposium of Robotics Research.*

Y.P. Leow, K.H. Low, W.K Loh, 2002, "Kinematic Modelling and Analysis of Mobile Robots with Omni-Directional Wheels", *Proceedings of the 7th International Conference on Control, Automation, Robotics and Vision, ICARCV 2002*, pp. 820-825.

J. Robinson, J.B. Holland, M.J.D. Hayes, and R.G. Langlois, 2005, "Velocity-level Kinematics of a Spherical Orienting Device Using Omni-directional Wheels", *CSME Transactions, Special Edition*, vol. 29, no. 4, pp. 691-700.

R.B. Roth and K.-M. Lee, 1995, "Design Optimization of a Three-Degree-of-Freedom Variable Reluctance Spherical Wrist Motor", *ASME J. Eng. Industry*, vol. 117, pp. 378-388.

A.L. Schwab, J.P. Meijaard, September 2006, "How to Draw Euler Angles and Utilize Euler Parameters", *Proceedings of ASME IDETC/CIE.*

D. Stewart, 1965, "A Platform with 6 Degrees of Freedom", *Proc. of the Institution of Mechanical Engineers*, vol. 180, Part 1, no. 15, pp. 371-378

A. Weiss, R.G. Langlois, M.J.D. Hayes, 2008, "The Effects of Dual-Row Omnidirectional Wheels on the Kinematics of the Atlas Spherical Motion Platform", to appear in *Mechanism and Machine Theory*.

F. Williams, E.R. Laithwaite, and G.F. Eastham, 1959, "Development and Design of Spherical Induction Motors", *Proc. IEEE*, vol. 47, pp. 471-484.